



ISSN 2305-1088

<https://jsasj.journals.ekb.eg>

JSAS 2023; 8(2): 282-295

Received: 09-12-2023

Accepted: 21-12-2023

Mazhar D A Mohamed**Doaa A Mohamed****Tarek H M Elsharouny**

Agricultural Microbiology Department

Faculty of Agriculture

Sohag University

Sohag

82524

Egypt

Bahig A El-Deeb

Botany and Microbiology Department

Faculty of Science

Sohag University

Sohag

82524

Egypt

Mohamed A Mosa

Nanotechnology & Advanced Nano-

Materials Laboratory (NANML)

Plant Pathology Research Institute

Agricultural Research Center

Giza

Egypt

Corresponding author:**Doaa A Mohamed**doaa.abdelhakeem@agr.sohag.edu.g

Biosynthesis and antimicrobial activity of copper oxide nanoparticles

Mazhar D A Mohamed, Bahig A El-Deeb, Doaa A Mohamed, Mohamed A Mosa and Tarek H M Elsharouny

Abstract

The development of simple, economical, and effective technologies to produce nanoparticles is a global priority. Microorganism-based biosynthesis methods developed as an environmentally conscious, pristine, and feasible alternative to conventional physical and chemical approaches. This research outlines the synthesis of copper oxide nanoparticles utilizing bacterial filtrated supernatant. The investigation focused on variables such as pH, copper concentration, and temperature. Optimal conditions for nanoparticle formation were identified at a neutral pH, 4 mM copper concentration, and 35°C. Characterization of the CuO NPs involved TEM, UV-Vis spectroscopy, XRD, and FTIR to examine their pure form, revealing a maximum particle size of 36.22 nm with spherical morphology. Evaluating the antimicrobial efficacy on pathogenic bacteria (*Staphylococcus aureus* and *Pseudomonas aeruginosa*) and plant pathogenic fungi (*Rhizoctonia solani* and *Fusarium solani*) through the well diffusion method affirmed the probable outcome of CuO-NPs as an efficient antimicrobial agent, supporting and validating prior assertions.

Keywords: Nanoparticles of copper oxide, TEM, FTIR, XRD, The antimicrobial activity.

INTRODUCTION

Nanotechnology is characterized by the examination, and production of substances within the dimensions ranging from 1 to 100 nm (Albanese *et al.*, 2012). Various methodologies, such as microwave, hydrothermal, electrochemical, photochemical, microemulsion, and chemical reduction methods, are employed to produce copper nanoparticles (Cu NPs). (Khodashenas and Ghorbani, 2014). The creation of metal nanoparticles through chemical and physical methods is widely recognized as posing risks, being expensive, and environmentally unfriendly. (Fouda *et al.*, 2019). Thus, it is crucial to create fast, inexpensive, environmentally acceptable, and easily scaled synthetic methods of producing metal nanoparticles via biological systems using microorganisms and plant extracts. Under challenging conditions, microorganisms are commonly understood to develop resistance to toxic substances through the conversion of poisonous ions of metal into non-toxic counterparts in the form of metal nanoparticles. (Bukhari *et al.*, 2021). Gram-positive bacteria, known as actinomycetes, are a varied group that is extensively distributed in various environments and commonly found in soil. Microorganisms, particularly actinomycetes, are recognized for generating a diverse range of distinctive secondary metabolic products (Han *et al.*, 2015). possessing antibacterial, antifungal, and antiviral properties (Sultanpuram *et al.*, 2015). Actinomycetes are widely considered promising candidates for synthesizing metal nanoparticles owing to their stability and polydispersity, making them robust contenders for the production of both intracellular and extracellular metal nanoparticles (Golinska *et al.*, 2014). *Streptomyces sp.* is a type of actinomycetes that is frequently utilized in the production of nanoparticles (Zonooz *et al.*, 2012), and it has been shown that it can create copper, silver, gold, manganese, and zinc nanoparticles (Omran, 2020) that have many applications across a multitude of fields. Copper nanoparticles find crucial applications in various fields (Ismail *et al.*, 2019), with copper oxide (CuO) gaining specific emphasis due to its distinctive attributes such as stability,

conductivity, catalytic activity, antibacterial, and anticancer characteristics. In contrast to pricier and more precious metals like gold and silver, copper oxide nanoparticles (CuO-NPs) are more accessible, cost-effective, and have the potential to serve as efficient antimicrobial agents. This has sparked increased interest in CuONPs (Singh *et al.*, 2023). The main goal of this research was to investigate the synthesis and characterization the nanoparticles of copper oxide through biological processes while also assessing their antimicrobial activity.

MATERIALS AND METHODS

Source of bacteria

Bacterial isolates were obtained from soil samples gathered at the New Sohag Experimental Farm, affiliated with the Faculty of Agriculture at Sohag University in Sohag, Egypt.

Media and chemicals

In this investigation, copper-resistant bacteria were isolated using nutrient agar and broth media. The media composition included five grams peptone, three grams yeast extract, and fifteen grams agar per liter of distilled water, adjusted to a pH of 7. Sterilization of the media was achieved by autoclaving at 121°C for 20 minutes, as per the methodology outlined by Taran *et al.* (2017). To specifically target copper-resistant bacteria, the media were supplemented with a 1 mL mole solution of $\text{CuSO}_4 \cdot 5\text{H}_2\text{O}$ during the isolation process.

Copper – resistant bacteria isolation

The bacteria with resistance to copper were isolated according to BT *et al.* (2019). with some modifications as follows: The enrichment culture method was utilized to isolate copper-resistant bacteria by the serial dilution plate method using nutrient agar medium amended with a 1 mM $\text{CuSO}_4 \cdot 5\text{H}_2\text{O}$ solution. 1 ml of the soil extract was diluted with sterilized distilled water (10^{-1} - 10^{-6}). A 1 ml aliquot from each dilution was evenly spread on agar plates and subsequently incubated at 30°C for a duration of 5 days. The emergence of brown zones surrounding various colonies on the culture plates indicated the successful isolation of copper-resistant bacteria. To confirm

that the brown coloration was not a result of bacterial physiological pigmentation activity, the colonies were re-streaked onto nutrient agar medium plates without $\text{CuSO}_4 \cdot 5\text{H}_2\text{O}$. The pure cultures of the isolated strains were preserved on slants of nutrient agar medium at 4°C for future use.

Identification of bacterial isolate

DNA extraction by the boiling Lysis method

To collect bacterial cells, 2 ml of each bacterial culture (10^9 cfu/ml) underwent centrifugation at $5000 \times g$ for 10 minutes. The resulting supernatant was disposed of, and the cell pellet from each isolate was reconstituted in 100 μl of sterile distilled water. Subsequently, this mixture was centrifuged at $15,000 \times g$ for 10 minutes, and the pellets were collected. After resuspending the pellets in another 100 μl of sterile distilled water, the suspension was heated to 100°C in a water bath for 10 minutes and then promptly cooled on ice.

Following this, the cooled suspension underwent centrifugation at $12,000 \times g$ for 1 minute. The resulting supernatant, containing DNA, was gathered and kept at -20°C for use as the template in PCR, following the procedure outlined by Queipo-Ortuño *et al.* (2008).

PCR reaction set-up:

In this process, two primers were employed: a forward primer (5'-AGAGTTTGATCCTGGCTCAG-3') and a reverse primer (5'-TACGGTTACCTTGTTACGACTT-3'). The amplification steps utilized 8 μL of template DNA, 1 μL of each primer, 1X buffer with Mg^{2+} , 1U of Taq DNA Polymerase (Promega, USA), and 0.2 mM dNTPs.

Nuclease-free water was added to adjust the reaction volume to 25 μL . The samples underwent 35 PCR cycles following this cycle profile: an initial denaturation at 94°C for 6 minutes, denaturation at 94°C for 45 seconds, primer annealing at 56°C for 45 seconds, extension at 72°C for 2 minutes, and a final elongation step at 72°C for 5 minutes. Subsequently, the PCR product was purified and subjected to complete sequencing (Kumar *et al.*, 2001).

Biosynthesis copper nanoparticles (CuO-NPs).

To facilitate the biosynthesis of CuO-NPs by a chosen strain, one ml of a recent isolate liquid culture was added into a 250-ml Erlenmeyer flask with 50 ml of sterilized nutrient broth medium. The flask underwent incubation in a rotary incubator shaker set at 35°C and 170 rpm for a duration of five days. Following the incubation period, the culture was subjected to centrifugation at 6000 rpm for 15 minutes using the Centurion Scientific Benchtop Centrifuge, model PRO-RESEARCH.K2015R.

The biomass of the isolate was harvested and underwent three washes with sterilized distilled water. Subsequently, 50 ml of sterilized distilled water was introduced to the sample. The flask was re-incubated under the same conditions. After the incubation, the culture was centrifuged at 6000 rpm for 15 minutes, and the resulting supernatants were employed for the green synthesis of CuO-NPs. In each 250 ml Erlenmeyer flask, 1 ml of 100 mM $\text{CuSO}_4 \cdot 5\text{H}_2\text{O}$ solution was combined with the supernatant from each isolate. The flasks were once again incubated in a rotary incubator shaker at 35°C and 170 rpm for five days, with observations made for any color change.

The supernatant in a 250-ml Erlenmeyer flask from the isolate without $\text{CuSO}_4 \cdot 5\text{H}_2\text{O}$ solution was used as a control. On the other hand, sterile media mixed with a 1 mM $\text{CuSO}_4 \cdot 5\text{H}_2\text{O}$ solution was used as a control to show that media components could not convert copper ions to CuONPs. No discernible color alteration occurred throughout the observation period. The outcomes concerning color changes were depicted and analyzed using UV-visible spectroscopy within the spectrum of 200–800 nm, following the methodology described by Fesharaki *et al.* (2010) and BT *et al.* (2019).

Characterization of bacterially synthesized CuO-NPs.

The particle size distribution (SPR) of CuO-NPs was examined using a Vis spectrophotometer, specifically the JASCO V-770 Spectrophotometer, following the method outlined by Manyasree *et al.* (2017) and Nabila and Kannabiran (2018). To explore the coating of biomolecules for CuO-NP stability, Fourier

transform infrared (FTIR) spectroscopy was conducted using a Bruker Alpha Platinum-attenuated total reflection spectrophotometer within the range of 400–4000 cm^{-1} , as per the approach described by Nabila and Kannabiran (2018).

Additionally, the dried powder of CuO-NPs underwent characterization by X-ray diffraction (XRD) using a Philips type Pw1840 instrument with Cu-K α radiation - ($\lambda = 1.50456$) within the range of (100 to 800), following the methodology outlined by Qamar *et al.* (2020). The morphology of CuO-NPs was investigated by placing the sample onto a carbon-coated copper TEM grid for transmission electron microscopy (HR-TEM) using a JEOL JEM-2100 instrument (Bian *et al.*, 2021).

The role of pH on the forming of nanoparticles

The influence of pH on the biosynthesis of CuO-NPs was investigated across various pH values (5, 6, 7, 8, and 9). Each sample underwent incubation in a rotary shaker at 35°C for a duration of 5 days at 170 rpm. Subsequently, cell-free supernatant was collected for the examination of CuO-NP synthesis using UV-Vis analysis, following the methodology outlined by Bukhari (2021).

Copper Concentration's Influence on Nanoparticle Production

CuSO₄·5H₂O concentrations of 0.5, 1, 1.5, 2, and 4 mM were added to a volume of 50 ml of cell-free supernatant and subjected to the same incubation conditions as mentioned earlier. The impact of CuSO₄·5H₂O concentration on the formation of CuO-NPs was assessed through UV-Vis analysis, following the methodology outlined by Shantkriti and Riani (2014).

Temperature Influence on Nanoparticle Production

The isolate's culture supernatants were adjusted with CuSO₄·5H₂O and incubated at four different temperatures: 4°C, 15°C, 25°C, 35°C, and 40°C. UV-Vis was used to investigate the production of CuO-NPs.

The assessment of the antimicrobial activity of nanoparticles

The antimicrobial activities of nanoparticles were studied using the well diffusion method (Alavi and Karimi, 2018) as follows:

Activity of CuO-NPs against pathogenic bacteria

The antibacterial activity was evaluated against pathogenic G⁺ bacteria (*Staphylococcus aureus*) and G⁻ bacteria (*Pseudomonas aeruginosa*), both obtained from the bacterial laboratory stock at the Dept. of Microbiology, Faculty of Agriculture, Sohag University, Sohag, Egypt. Nutrient agar plates were inoculated with 100 μL culture of each test bacteria.

Small wells with a diameter of 6 mm were created in the agar plates using a sterilized cork borer. The wells were filled with different concentrations (25, 50, 75, and 100 μl) of each nanoparticle sample. 100 μl of the (CuSO₄·5H₂O) solution and 100 μl of the cultures of bacterial strains were used as controls. All plates were then incubated for 24 hours at 35°C. The areas of inhibition for each sample were measured in millimeters, following the approach outlined by Alavi and Karimi (2018).

Antifungal activity

The activity of nanoparticles as antifungal was evaluated toward certain plant pathogenic fungi, namely *Fusarium solani* and *Rhizoctonia solani*. The testing was conducted using the agar-well diffusion method, and the fungal strains were sourced from the Department of Plant and Microbiology, Faculty of Science, Sohag University, Sohag, Egypt.

Firstly, the tested fungi were cultured in 5 ml of distilled water for 3 hours. Potato D-glucose Agar (PDA) plates were formulated by preparing the Potato D-glucose Agar (PDA) media, which comprised 1000 mL of distilled water, 20 g/L agar, 200 g of potatoes, and 20 g of D-glucose, following the procedure outlined by Viet *et al.* in 2016. Subsequently, the plates were inoculated with a 100 μL culture of each fungal isolate.

The plates were incubated for 15 minutes to allow for culture absorption on agar plates. The wells of 6 mm diameter were made into the agar plates with a sterilized cork borer. The wells were filled

with different concentrations (50, 75, and 100 ul) of each nanoparticle sample. 100 ul of the $\text{CuSO}_4 \cdot 5\text{H}_2\text{O}$ solution and 100 ul of the cultures of bacterial strains were used as controls. For 5 days, every plate was left to incubate at 29°C. Each sample's inhibitory zones were measured in millimeters (Rajeshkumar and Rinitha, 2018; Tahir *et al.*, 2022).

RESULTS AND DISCUSSION

Bacterial Identification

Molecular techniques were employed to validate and confirm the identification of the *Streptomyces* strain at the species level. The primary method involved conducting 16S rRNA gene phylogeny studies. Amplicons, representing the 16S rRNA genes and measuring 1240 bp, were obtained. BLASTN was used to compare these amplicons to the GenBank database at the National Center for Biotechnology Information (NCBI) for further confirmation of the bacterial identification.

This isolate was found to belong to the *Streptomyces* species with a homology level of 99%. The strain was identified as *Streptomyces thermolilacinus* by alignment of our sequence to the sequence of the *Streptomyces* strain.

The first isolate's 16S rRNA gene sequence exhibited substantial sequence similarity with members of the genus *Streptomyces*, including *Streptomyces* sp strain GB24 (JX965401) (99%), *Streptomyces fradiae* (FJ486352) (99%), and *Streptomyces thermolilacinus* (AB184585) (99%).

According to the obtained results, Strain was identified as *Streptomyces thermolilacinus* A.Hakim. The Accession number (OR573793.1) and the fragmentary 16s rRNA gene sequencing of isolate 3 submitted in genbank. Based on 16s rRNA gene the isolate was identified as *Streptomyces thermolilacinus* A.Hakim. Bacteria; Actinobacteria; Streptomycetales; Streptomycetaceae; *Streptomyces* (Gurtler and Stanisich, 1996).

Analyzing the biosynthesis of CuONPs using UV-Vis

The cell-free supernatant was combined with an aqueous solution of copper sulfate [$\text{CuSO}_4 \cdot 5\text{H}_2\text{O}$]

and incubated at 35°C for 5 days. The transition in color from light brown to dark brown signifies the synthesis of CuO-NPs (Fig. 1). This observation aligns with the findings of Arif (2023), who demonstrated a similar color change to brown when CuCl_2 solution was introduced to the *A. niger* extract filtrate solution, indicating the biosynthesis of CuO-NPs.

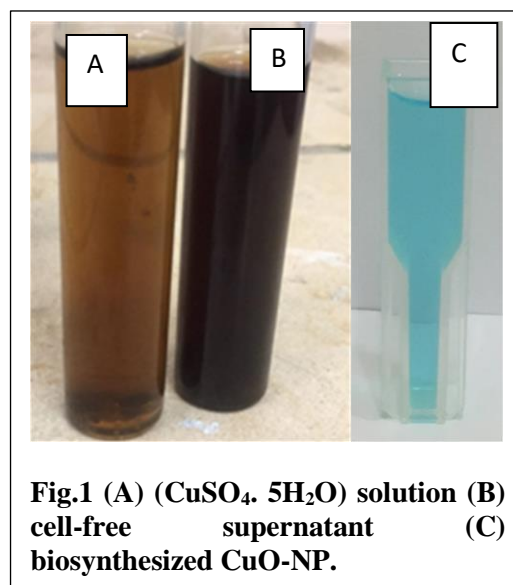


Fig.1 (A) ($\text{CuSO}_4 \cdot 5\text{H}_2\text{O}$) solution (B) cell-free supernatant (C) biosynthesized CuO-NP.

As per the UV-Vis spectroscopy results, the presence of CuONPs in the sample is indicated by the Surface Plasmon Resonance (SPR) absorption peak at 569 nm (Figure 2). The specific location of the SPR band can vary based on the characteristics of individual particles, including size, shape, and capping agents (Mott *et al.*, 2007). This finding is consistent with the work of Ghorbani *et al.* (2015), who noted a SPR band for CuO NPs biosynthesized by *Salmonella typhimurium* at 565 nm.

X-ray diffraction (XRD) of CuONPs

As shown in Fig. 3, the crystal structure of the synthesized CuONPs nanoparticles was investigated by XRD. The CuO nanoparticles that were created showed the strongest peak at a 2θ of around 35.5°, 36.4°, 38.7°, 48.8°, and 61.5°, which correspond to (002), (111), (200), (202), and (113) diffraction planes for the Cu_2ONPs ' cubic phase structure, respectively. Only a pure Cu_2ONP phase can develop when all other phase peaks disappear.

Additionally, the higher intensity observed in the (111) peak signifies a superior level of crystallization, consistent with the Cu₂O powder peaks found in the International Centre of Diffraction Data Card (JCPDS file no. 05-0667). The calculated particle size from the highest diffraction peak (111) was determined to be approximately 35.1 nm. The presence of well-defined structural peaks in the XRD patterns and crystallite sizes below 100 nm indicate the nanocrystalline nature of both crude and calcined CuONPs. The current findings align with those reported by Das *et al.* (2013) and Padil and

Černík (2013), who characterized CuONPs using XRD and identified diffraction peaks at $2\theta = 32.47^\circ, 35.49^\circ, 38.68^\circ, 48.65^\circ, 53.36^\circ, 58.25^\circ,$ and 61.45° , attributing them to reflection lines of monoclinic CuO nanoparticles. Additionally, Kamel *et al.* (2022) investigated fabricated nanoparticles through XRD, noting that the most intense peak of the synthesized Cu₂O nanoparticles appeared at approximately 36.43° , corresponding to the (111) diffraction plane of the cubic phase of Cu₂O.

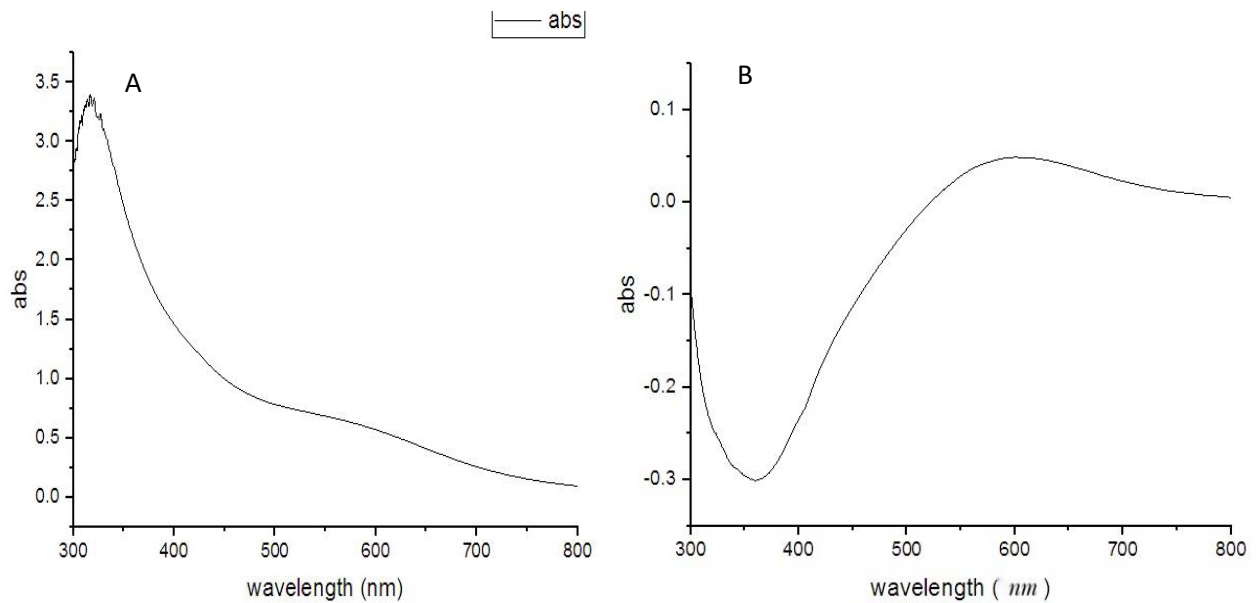


Fig .2 UV-visible absorption spectra analysis (A) control(B) CuO NPS synthesized using supernatant of 72 h old culture supplemented with 1 mM CuSO₄ solution and incubated statically.

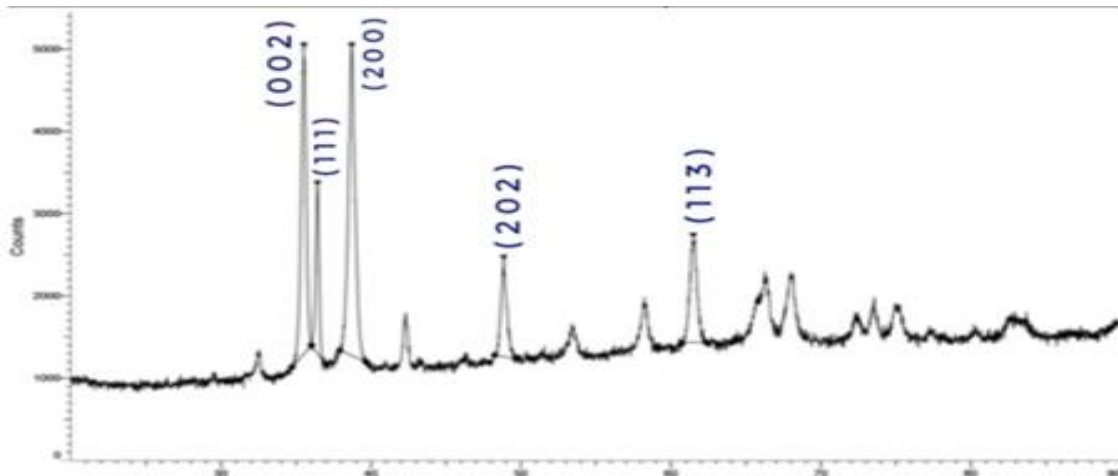


Fig.3. XRD analysis of Cu₂O nanoparticles.

FTIR study of Copper Oxide Nanoparticles produced

The study showed different characteristic peaks in the FTIR measurement, with the supernatant of the isolate only showing different peaks at 583.87 cm^{-1} , 911.00 cm^{-1} , 1011.51 cm^{-1} , 1054.90 cm^{-1} , 1636.03 cm^{-1} , and 3267.19 cm^{-1} . For the synthesized CuONPs, different characteristic peaks are observed in the FTIR measurement at 575.39 cm^{-1} , 604.25 cm^{-1} , 1011.51 cm^{-1} , 1051.13 cm^{-1} , 1224.29 cm^{-1} , 1329.38 cm^{-1} , 1457.77 cm^{-1} , 1637.46 cm^{-1} , and 3267.18 cm^{-1} .

Moreover, the robust peak at 3267.18 cm^{-1} was associated with the hydroxyl groups within the protein of the capping agent on the surface of CuONPs. Additionally, the peak observed at 1636.03 cm^{-1} indicated stretching vibrations of amide and ester groups in the C=O direction, and C=C aromatic ring stretching vibrations were noted at 1457.77 cm^{-1} . Furthermore, the peak at 1329.38 cm^{-1} was assigned to the C-N amide III band. The absorption peak at 1224.29 cm^{-1} is indicative of molecules containing C-O bonds as a result of stretching.

The bands at 1051.13 cm^{-1} and 1011.51 cm^{-1} attributed to the C-N bond of the amine group. The bands at 575.39 cm^{-1} and 604.25 cm^{-1} assigned to the Cu-O bond in this investigation confirmed the synthesis of CuONPs (Fig. 4). Therefore, it is achievable that biological molecules perform two separate tasks that contribute to the formation and stability of copper

oxide nanoparticles in an aqueous medium (Rapachi *et al.*, 2023). These results agree with the organic functional groups contributed to CuONPs synthesis that were discovered by Nabila and Kannabiran (2018), Hassan *et al.* (2019), and El-Saadony *et al.* (2020).

CuONPs TEM analysis

Transmission Electron Microscopy (TEM) is a crucial technique that offers detailed insights into the dimension, distribution, and average size of nanoparticles. In the investigation of biologically generated CuO nanoparticles, TEM was employed to examine their size, shape, and morphology.

As depicted in (Fig. 5) and the graph of size distribution of CuO-NPs (Fig. 6), the results indicate a remarkably uniform size for the synthesized CuO-NPs, exhibiting an average size of 36.22 nm and an irregular spherical shape.

The small particle aggregates have a thin organic coating applied to them that serves as a capping organic agent. That might explain why the nanoparticles exhibit excellent dispersion, even at the macroscopic level, within the bio-reduced aqueous solution.

These findings align with the results reported by Mali *et al.* (2019) and Zhao *et al.* (2022), both of whom synthesized CuO-NPs and observed spherical shapes with particle diameters of $10\text{--}30\text{ nm}$ and 6.44 nm , respectively.

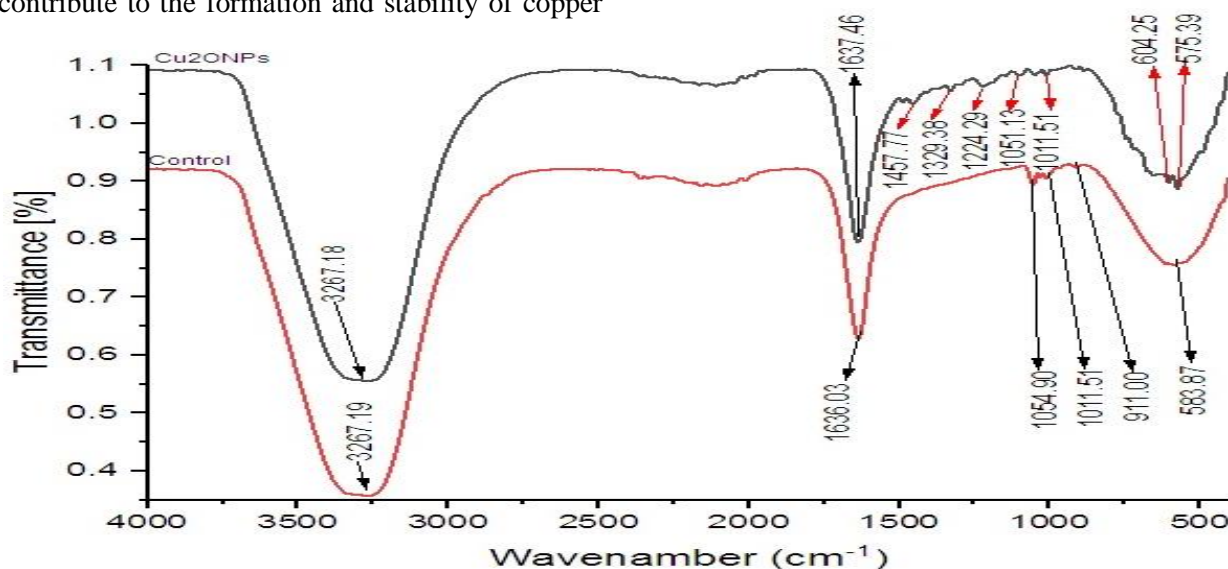


Fig.4 FTIR analysis of biogenic CuO nanoparticles.

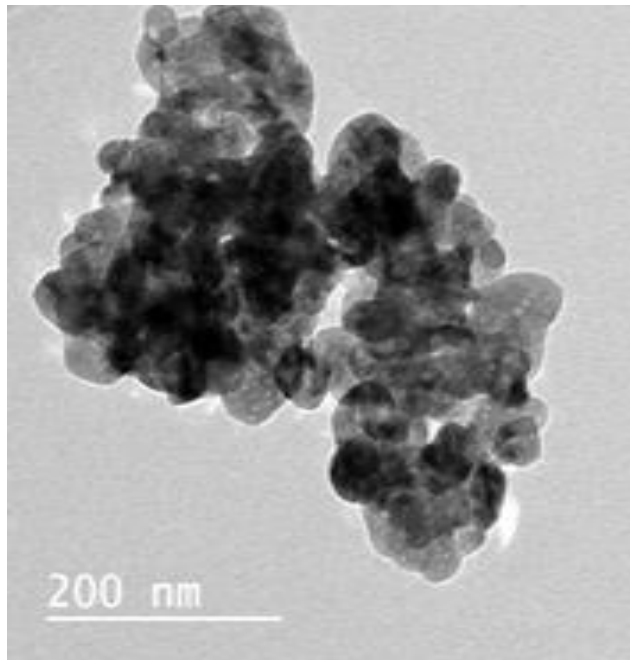


Figure 5 shows a TEM picture of Cu₂O nanoparticles

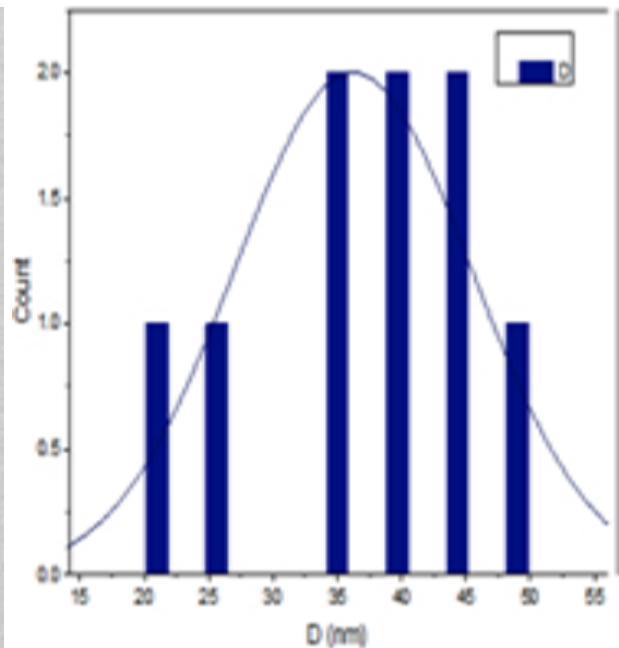


Figure6: Particle-size distribution of produced nanoparticles

The impact of pH on the biosynthesis of copper oxide nanoparticles.

Results showed that, when comparing the reactions through the visual assays and the SPR obtained through UV-Vis spectra, the dark brown color of the solution was decreased by increasing medium alkalinity, where the extracellular CuO-NPs were formed at all pH values with optimum formation at pH 7 (Fig. 7). Hence, it was determined that pH 7 was optimal for the biosynthesis of CuO-NPs.

These findings are similar to those previously published by Ghareib *et al.* (2018), who concluded that the biosynthesis of CuO-NPs by *Aspergillus fumigatus* was achieved at a neutral pH. However, both alkaline and acidic pH levels may affect the biosynthesis of CuO-NPs.

Effect of Copper Concentration on the biosynthesis of CuONPs

According to the results presented in Figure 8, the Surface Plasmon Resonance (SPR) absorption of CuONPs increased with the rise in substrate concentration from 0.5 to 4 mM, reaching its maximum absorption at 4 mM of CuSO₄.5H₂O and exhibiting SPR absorption at 613 nm. This observation suggests an increase in the production of CuO-NPs as the reaction progresses, as the intensity of the surface plasmon peak is directly proportional to the density of CuO-NPs in the

reaction mixture. This finding is in line with the findings of Honary *et al.* (2012), who noted that high concentrations of salt ions resulted in larger particle sizes and a broader size distribution of synthesized nanoparticles.

Effect of Temperature on the biosynthesis of CuO-NPs

As per the results, the formation of CuO-NPs increased with the temperature rising to 35°C, and a significant decrease in absorbance was observed at 40°C (Fig. 9). The accelerated synthesis of CuO-NPs could be a direct consequence of the temperature's impact on a key enzyme produced in the culture of *Streptomyces thermolilacinus*.

The rate of CuO-NP formation was associated with the incubation temperature of the reaction mixture, with higher temperature levels promoting rapid particle growth. In a comparable investigation, El-Saadony *et al.* (2020) documented that the most favorable temperature for the synthesis of copper oxide nanoparticles (CuO-NPs) by *Pseudomonas fluorescens* MAL2 was 35°C. They observed negligible production of CuO-NPs at temperatures exceeding 40°C.

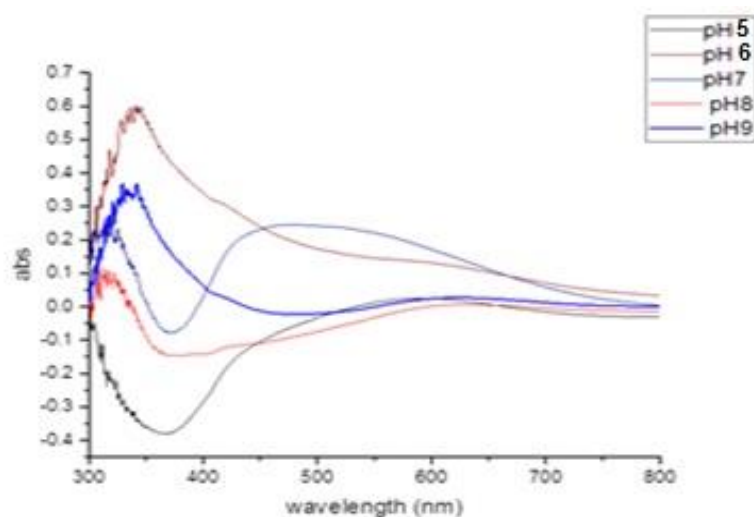


Fig.7. Influence of Various pH Levels on the Formation of CuONPs.

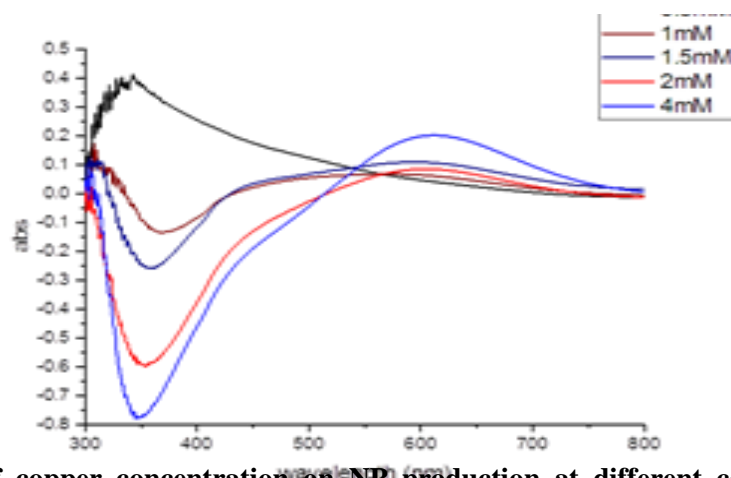


Fig. 8. Effect of copper concentration on NP production at different concentrations of CuSO₄ solution.

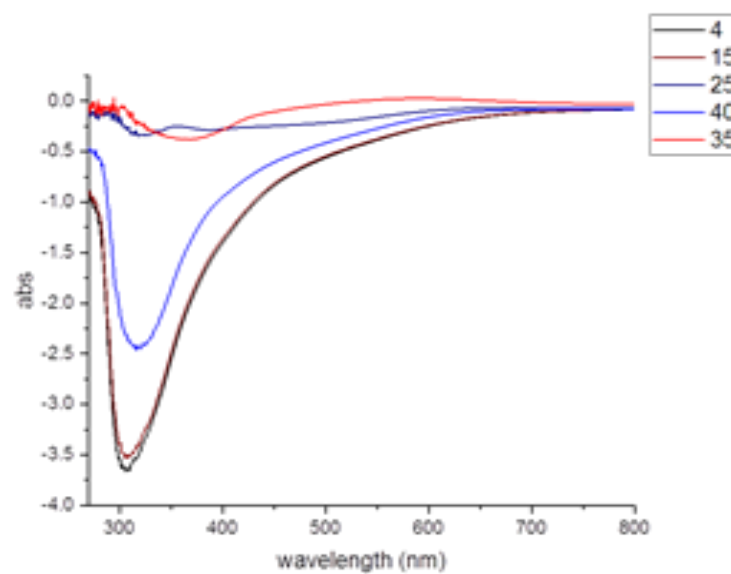


Fig. 9 Effect of different temperature values (4°C, 15°C, 25°C,35°C and 40°C) on Cu₂O NPs formation.

Antibacterial Activity of CuONPs

As per the findings of this study, copper oxide nanoparticles (CuO-NPs) exhibited significant antibacterial activity against the tested bacterial strains. Based on the inhibition zone (ZOI), the antibacterial activity of CuO-NPs against *P.aeruginosa* exhibited inhibition zone diameter about 19 mm, while *S.aureus* recorded a zone of inhibition about 18 mm in diameter. Figure 10 depicts the antibacterial activity of biosynthesized CuO-NPs across tested bacterial strains.

The antibacterial efficacy of CuO-NPs can be attributed to several mechanisms, as indicated by their corresponding ZOI values. These mechanisms include the deposition of nanoparticles, release of Cu^{2+} ions from the nanostructure, generation of reactive oxygen species on the nanostructure's surface, and physical contact between the particle surface and the biological target. The interaction between the bacterial cells and nanomaterial occurs through these various modes, resulting in the formation of a visible ZOI.

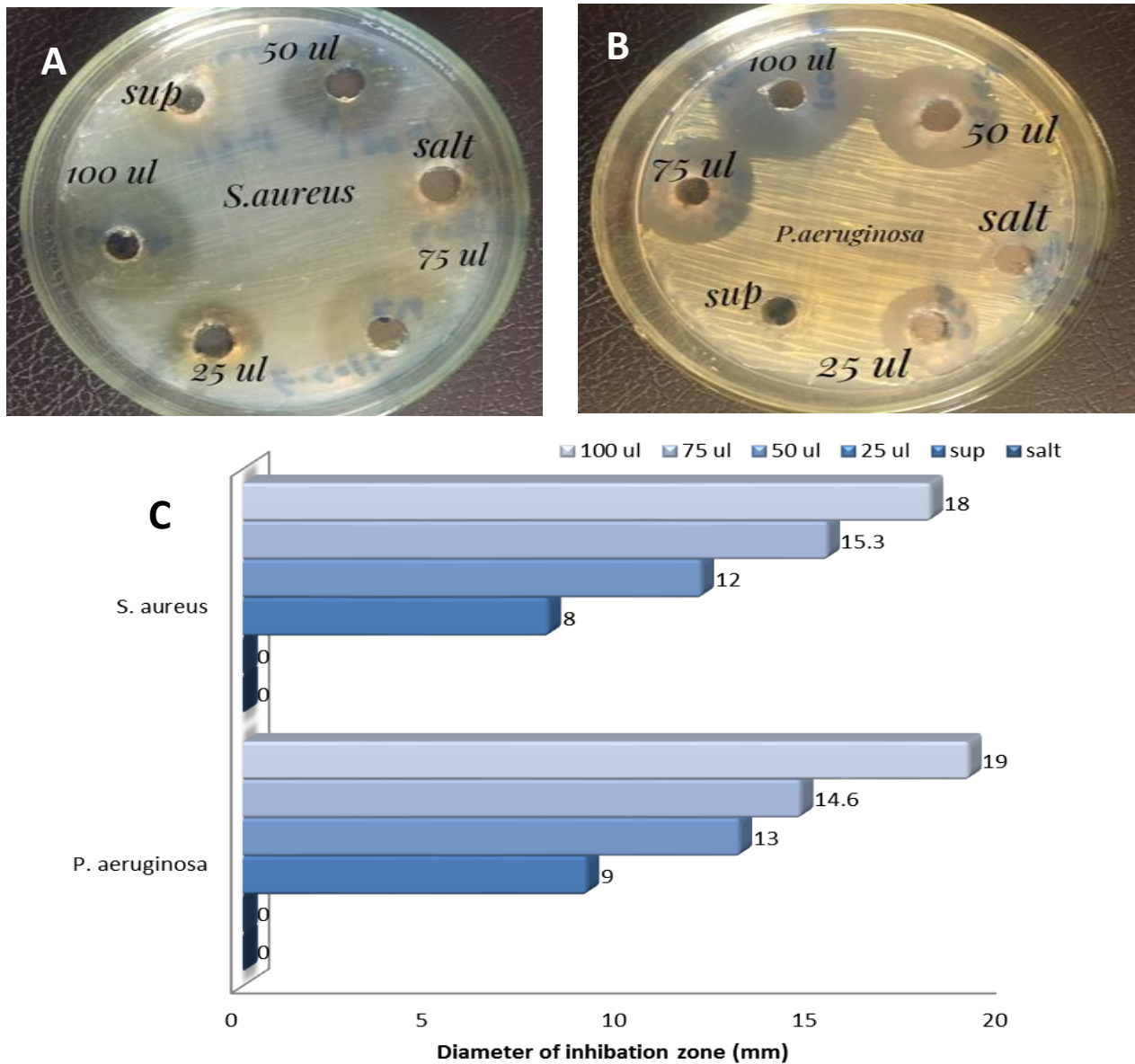


Fig. 10. Antibacterial activities of Cu₂O nanoparticles at different concentration against (A) *P. aeruginosa* (B) *S. aureus* (C) Biosynthesized CuO-NPs show antibacterial properties against bacterial strains.

Antifungal Activity of CuO-NPs

The results of this study demonstrated a highly substantial impact of synthetic copper oxide nanoparticles on the mycelium growth of the fungus *F. solani* with an inhibition zone of diameter equal to 18 mm, while inhibition of the zone of *R. solani* was observed with a diameter equal to 14 mm at the same concentration. The lowest levels of growth inhibition were observed at concentrations of 50 ul of synthesized copper oxide nanoparticles, with inhibition zones of

diameter equal to 4.3 and 4 mm for *F. solani* and *R. solani*, respectively (Fig. 10).

The antifungal activity of copper oxide nanoparticles can be elucidated through a "contact killing" mechanism. This mechanism suggests that copper provides a surface for eliminating microorganisms, such as fungi and bacteria, by inducing significant damage to the cell membrane, enlarging cell vacuoles, and causing cell disappearance (Ma *et al.*, 2022).

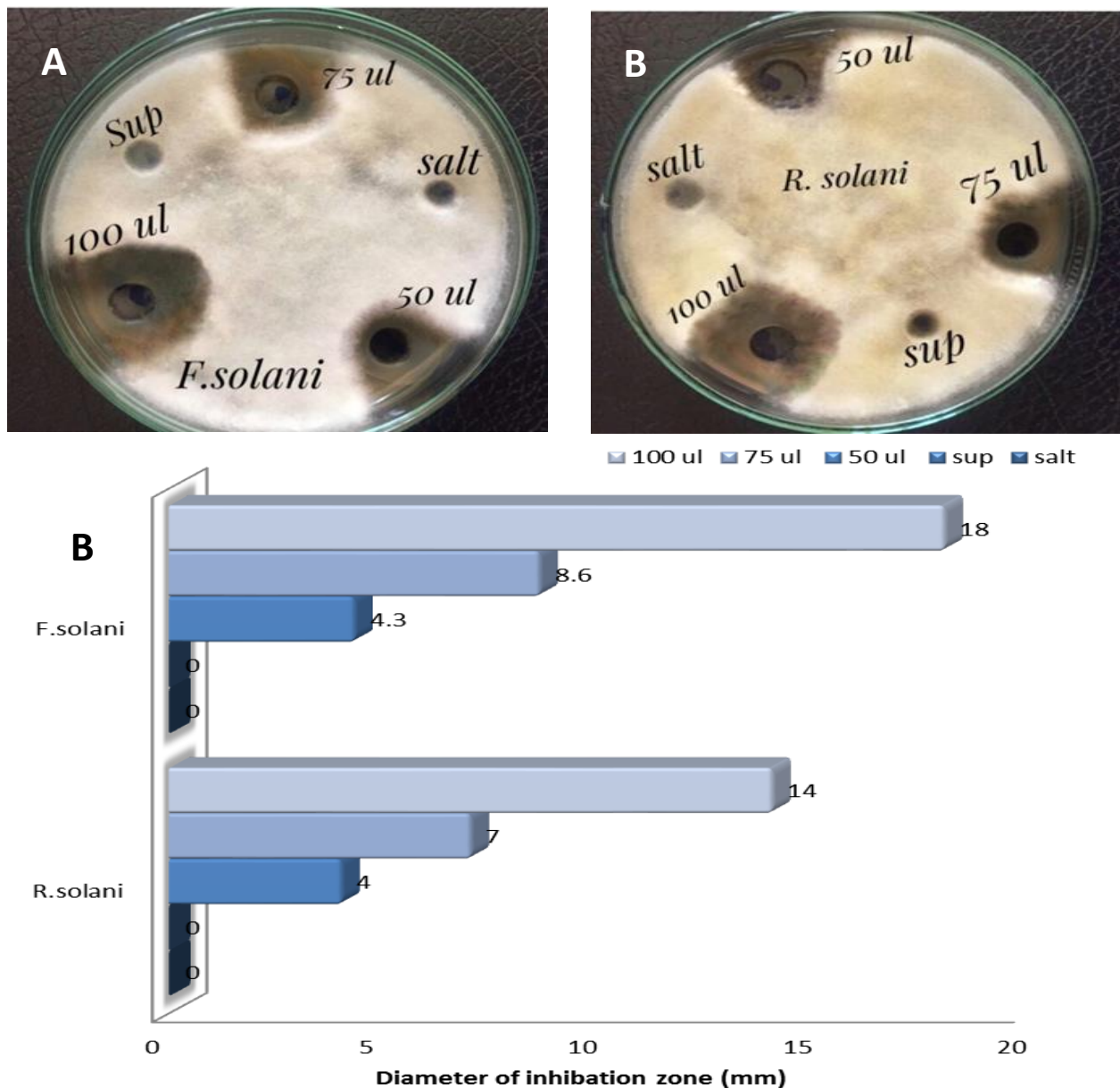


Fig.11. Antifungal activities of Cu₂O nanoparticles at different concentration against (A)*F. solani* (B) *R. solani* (C) Antifungal activity of biosynthesized CuO- NPs against fungal strains.

CONCLUSION

Finally, we present a straightforward, swift, and environmentally friendly method for producing CuO-NPs with remarkable antibacterial properties. The synthesized nanoparticles exhibit high stability and a monoclinic structure, with the majority falling within a size range of 36.22 nm in diameter, as determined through various methodologies assessing size, shape, composition, and stability. The encouraging results suggest that CuO-NPs could serve as an effective agent against pathogenic microorganisms. The findings of this study indicate that environmentally friendly CuO-NPs hold great promise and could find applications in diverse fields, including biomedicine and agriculture.

REFERENCES

- Alavi, M., and Karimi, N. (2018). Characterization, antibacterial, total antioxidant, scavenging, reducing power and ion chelating activities of green synthesized silver, copper and titanium dioxide nanoparticles using *Artemisia haussknechtii* leaf extract. *Artificial cells, nanomedicine, and biotechnology*, 46(8), 2066-2081.
- Albanese, A., Tang, P. S., and Chan, W. C. (2012). The effect of nanoparticle size, shape, and surface chemistry on biological systems. *Annual review of biomedical engineering*, 14, 1-16.
- Arif, A. I (2023). Biosynthesis of copper oxide nanoparticles using *Aspergillus niger* extract and their antibacterial and antioxidant activities. *Eurasian Chemical Communications*, 5(7), 598-608. Doi: 10.22034/ecc.2023.384414.1600.
- BT, A. E., RF, G., Kh A, A. T., and AA, H. (2019). Biosynthesis of Copper nanoparticles using bacterial supernatant optimized with certain agro-industrial byproducts. *Novel Research in Microbiology Journal*, 3(6), 558-578.
- Bukhari, S. I., Hamed, M. M., Al-Agamy, M. H., Gazwi, H. S., Radwan, H. H., and Youssif, A. M. (2021). Biosynthesis of copper oxide nanoparticles using *Streptomyces* MHM38 and its biological applications. *Journal of Nanomaterials*, 2021.
- Das, D., Nath, B. C., Phukon, P., and Dolui, S. K. (2013). Synthesis and evaluation of antioxidant and antibacterial behavior of CuO nanoparticles. *Colloids and Surfaces B: Biointerfaces*, 101, 430-433.
- El-Saadony, M. T., Abd El-Hack, M. E., Taha, A. E., Fouda, M. M., Ajarem, J. S., N. Maooda, S., and Elshaer, N. (2020). Ecofriendly synthesis and insecticidal application of copper nanoparticles against the storage pest *Tribolium castaneum*. *Nanomaterials*, 10(3), 587.
- Fesharaki, P. J., Nazari, P., Shakibaie, M., Rezaie, S., Banoee, M., Abdollahi, M., and Shahverdi, A. R. (2010). Biosynthesis of selenium nanoparticles using *Klebsiella pneumoniae* and their recovery by a simple sterilization process. *Brazilian Journal of Microbiology*, 41, 461-466.
- Fouda, A., Abdel-Maksoud, G., Abdel-Rahman, M. A., Salem, S. S., Hassan, S. E. D., and El-Sadany, M. A. H. (2019). Eco-friendly approach utilizing green synthesized nanoparticles for paper conservation against microbes involved in biodeterioration of archaeological manuscript. *International Biodeterioration & Biodegradation*, 142, 160-169.
- Ghareib, M., Tahon, M. A., Abdallah, W. E., and Tallima, A. (2018). Green biosynthesis of copper oxide nanoparticles using some fungi isolated from the Egyptian soil. *Int. J. Res. Pharm. Nano Sci*, 7(4), 119-128.
- Ghorbani, H. R., Fazeli, I., & Fallahi, A. A. (2015). Biosynthesis of copper oxide nanoparticles using extract of *E. coli*. *Orient J Chem*, 31(1), 515-517.
- Golinska, P., Wypij, M., Ingle, A. P., Gupta, I., Dahm, H., and Rai, M. (2014). Biogenic synthesis of metal nanoparticles from actinomycetes: biomedical applications and cytotoxicity. *Applied microbiology and biotechnology*, 98, 8083-8097.
- Han, L., Zhang, G., Miao, G., Zhang, X., and Feng, J. (2015). *Streptomyces kanasensis* sp. nov., an antiviral glycoprotein producing actinomycete isolated from forest soil around

- kanas lake of China. *Current microbiology*, 71, 627-631.
- Honary, S., Barabadi, H., Gharaei-Fathabad, E., and Naghibi, F. (2012). Green synthesis of copper oxide nanoparticles using *Penicillium aurantiogriseum*, *Penicillium citrinum* and *Penicillium waksmanii*. *Dig J Nanomater Bios*, 7(3), 999-1005.
- Ismail, M., Gul, S., Khan, M. I., Khan, M. A., Asiri, A. M., and Khan, S. B. (2019). Green synthesis of zerovalent copper nanoparticles for efficient reduction of toxic azo dyes congo red and methyl orange. *Green processing and synthesis*, 8(1), 135-143.
- Kamel, S. M., Elgobashy, S. F., Omara, R. I., Derbalah, A. S., Abdelfatah, M., El-Shaer, A., and Elsharkawy, M. M. (2022). Antifungal activity of copper oxide nanoparticles against root rot disease in cucumber. *Journal of Fungi*, 8(9), 911.
- Khodashenas, B., and Ghorbani, H. R. (2014). Synthesis of copper nanoparticles: An overview of the various methods. *Korean Journal of Chemical Engineering*, 31, 1105-1109.
- Kumar, S., Tamura, K., Jakobsen, I. B., and Nei, M. (2001). MEGA2: molecular evolutionary genetics analysis software. *Bioinformatics*, 17(12), 1244-1245.
- Ma, X., Zhou, S., Xu, X., and Du, Q. (2022). Copper-containing nanoparticles: Mechanism of antimicrobial effect and application in dentistry-a narrative review. *Frontiers in Surgery*, 9, 905892.
- Mali, S. C., Raj, S., and Trivedi, R. (2019). Biosynthesis of copper oxide nanoparticles using *Enicostemma axillare* (Lam.) leaf extract. *Biochemistry and biophysics reports*, 20, 100699.
- Manyasree, D., Peddi, K. M., and Ravikumar, R. (2017). CuO nanoparticles: synthesis, characterization and their bactericidal efficacy. *Int J Appl Pharmaceut*, 9(6), 71-74.
- Melkamu, W. W., and Feleke, E. G. (2022). Green Synthesis of Copper Oxide Nanoparticles Using Leaf Extract of *Justicia Schimperiana* and their Antibacterial Activity.
- Mott, D., Galkowski, J., Wang, L., Luo, J., and Zhong, C. J. (2007). Synthesis of size-controlled and shaped copper nanoparticles. *Langmuir*, 23(10), 5740-5745.
- Nabila, M. I., and Kannabiran, K. (2018). Biosynthesis, characterization and antibacterial activity of copper oxide nanoparticles (CuO NPs) from actinomycetes. *Biocatalysis and agricultural biotechnology*, 15, 56-62.
- Omran, B. A., (2020). Prokaryotic microbial synthesis of nanomaterials (the world of unseen). *Nanobiotechnology: A Multidisciplinary Field of Science*, 37-79.
- Padil, V. V. T., and Černík, M. (2013). Green synthesis of copper oxide nanoparticles using gum karaya as a biotemplate and their antibacterial application. *International journal of nanomedicine*, 889-898.
- Qamar, H., Rehman, S., Chauhan, D. K., Tiwari, A. K., and Upmanyu, V. (2020). Green synthesis, characterization and antimicrobial activity of copper oxide nanomaterial derived from *Momordica charantia*. *International Journal of Nanomedicine*, 15, 2541.
- Queipo-Ortuño, M. I., De Dios Colmenero, J., Macias, M., Bravo, M. J., and Morata, P. (2008). Preparation of bacterial DNA template by boiling and effect of immunoglobulin G as an inhibitor in real-time PCR for serum samples from patients with brucellosis. *Clinical and Vaccine Immunology*, 15(2), 293-296.
- RajeshKumar, S., and Rinitha, G. (2018). Nanostructural characterization of antimicrobial and antioxidant copper nanoparticles synthesized using novel *Persea americana* seeds. *OpenNano*, 3, 18-27.
- Rapachi, D., de M. Peixoto, C. R., Pavan, F. A., and Gelesky, M. A. (2023). Metallic Nanoparticles Biosynthesized by Phenolic-Rich Extracts: Interaction, Characterization and Application. *Journal of Cluster Science*, 1-15.
- Rasool, U., and Hemalatha, S. J. M. L. (2017). Marine endophytic actinomycetes assisted synthesis of copper nanoparticles (CuNPs): Characterization and antibacterial efficacy against human pathogens. *Materials Letters*, 194, 176-180.
- Sampath, M., Vijayan, R., Tamilarasu, E., Tamilselvan, A., & Sengottuvelan, B. (2014).

- Green synthesis of novel jasmine bud-shaped copper nanoparticles. *Journal of Nanotechnology*, 2014.
- Shantkriti, S., and Rani, P. (2014). Biological synthesis of copper nanoparticles using *Pseudomonas fluorescens*. *Int J Curr Microbiol App Sci*, 3(9), 374-383.
- Shende, S., Ingle, A. P., Gade, A., and Rai, M. (2015). Green synthesis of copper nanoparticles by *Citrus medica* Linn. (Idilimbu) juice and its antimicrobial activity. *World Journal of Microbiology and Biotechnology*, 31, 865-873.
- Singh, D., Jain, D., Rajpurohit, D., Jat, G., Kushwaha, H. S., Singh, A., and Upadhyay, S. K. (2023). Bacteria assisted green synthesis of copper oxide nanoparticles and their potential applications as antimicrobial agents and plant growth stimulants. *Frontiers in Chemistry*, 11, 1154128.
- Sultanpuram, V. R., Mothe, T., and Mohammed, F. (2015). *Nocardioideosolisilvae* sp. nov., isolated from a forest soil. *Antonie Van Leeuwenhoek*, 107, 1599-1606.
- Taran, M., Rad, M., and Alavi, M. (2017). Antibacterial activity of copper oxide (CuO) nanoparticles biosynthesized by *Bacillus* sp. FU4: optimization of experiment design. *Pharmaceutical Sciences*, 23(3), 198-206.
- Viet, P. V., Nguyen, H. T., Cao, T. M., and Hieu, L. V. (2016). *Fusarium* antifungal activities of copper nanoparticles synthesized by a chemical reduction method. *Journal of Nanomaterials*, 2016.
- Zhao, H., Maruthupandy, M., Al-mekhlafi, F. A., Chackaravarthi, G., Ramachandran, G., and Chelliah, C. K. (2022). Biological synthesis of copper oxide nanoparticles using marine endophytic actinomycetes and evaluation of biofilm producing bacteria and A549 lung cancer cells. *Journal of King Saud University-Science*, 34(3), 101866.
- Zonooz, N. F., Salouti, M., Shapouri, R., & Nasseryan, J. (2012). Biosynthesis of gold nanoparticles by *Streptomyces* sp. ERI-3 supernatant and process optimization for enhanced production. *Journal of Cluster Science*, 23, 375-382.

الملخص العربي

التكوين الحيوي والنشاط المضاد للميكروبات لجزيئات أكسيد النحاس النانوية

مظهر دسوقي على محمد¹، بهيج الديب²، دعاء عبد الحكيم محمد¹، محمد موسى³، طارق حسن موسى الشاروني¹
 أقسام الميكروبيولوجيا الزراعية، كلية الزراعة، جامعة سوهاج، مصر.
² قسم النبات والميكروبيولوجي، كلية العلوم، جامعة سوهاج، مصر.
³ معمل تكنولوجيا النانو والمواد النانوية المتقدمة (NANML)، معهد بحوث أمراض النبات، مركز البحوث الزراعية، الجيزة، مصر.

في جميع أنحاء العالم يتم التركيز علي تطوير طرق بسيطة، فعالة وقليلة التكلفة لتكوين جزيئات النانومعدنية . التكوين الحيوي لهذه الجزيئات باستخدام الكائنات الحية الدقيقة آمن بيئياً وقابل للتطبيق مقارنة بالطرق الكيميائية والفيزيائية. تصف هذه الدراسة إنتاج جزيئات أكسيد النحاس النانوية (CuO-NPs) باستخدام مزارع الخلايا البكتيرية . تم دراسة عدة عوامل مثل الأس الهيدروجيني وتركيز النحاس ودرجة الحرارة وكانت الظروف المثلى لتكوين جزيئات النانومعدنية هي درجة حموضة المعتدلة ، 4 ملي مولار من تركيز النحاس عند 35 درجة مئوية. تم توصيف CuO-NPs باستخدام التحليل الطيفي للأشعة المرئية وفوق البنفسجية، واستخدمت تقنيات FTIR و XRD و TEM لدراسة الشكل النقي لـ CuO-NPs. وجد أن الحجم الأمثل للجسيمات كان 36.22 نانومتر كروية الشكل . تم تحديد النشاط المضاد للميكروبات لـ CuO-NPs باستخدام well diffusion method المضاد للبكتيريا المسببة للأمراض البشرية مثل *Staphylococcus aureus* و *Pseudomonas aeruginosa* والفطريات الممرضة للنبات مثل *Rhizoctonia solani* و *Fusarium solani*. تؤكد نتائج هذه الدراسة على أنه يمكن استخدام CuO-NPs كعامل فعال مضاد للميكروبات.